Guided Wave Technology

Narrowband Microwave Bandpass Filter Design by Coupling Matrix Synthesis

Morten Hagensen

Guided Wave Technology ApS, Hilleroed, Denmark

1. Introduction

In recent years advances within particularly two fields have had a major impact on how filters are designed today. One is the advent of powerful electromagnetic (EM) software, which provides results that are close to measurements. Analysis and optimization of complete filters is, however, even today often too resource and time consuming to be useable in practice. Methods which separate the entire structure into discrete components for individual EM analysis are therefore often employed [1].

The other field which has had a major impact on filter design methods is advances within the coupling matrix representation of microwave filter circuits. The coupling matrix concept was introduced in the 1970s, but lately general methods have been introduced for its synthesis [2], and the coupling matrix concept has been reformulated also to accommodate couplings directly from the source and the load to internal resonators [3].
The coupling matrix representation of bandpass filters is convenient, since with matrix operations it is possible to transform between topologies whereby the best suited topology for a given problem may be found. The recent coupling matrix formulation leads to more accurate determination of practical filter characteristics, and highly complex filters with multiple non-adjacent couplings are now easily synthesized.

Even though a large number of articles dealing with coupling matrix synthesis has recently been – and is being – published, almost none of them go into details about how to convert the synthesized matrices into physical filters. In this article, a practical filter design using coupling matrix synthesis and simple 3-D EM simulation techniques is demonstrated. Even though EM solvers in this article are used for the designs, the adopted methods may be applied even without EM solvers available. In that case, a couple of test circuits must be manufactured. Emphasis is made on practical approaches and it is demonstrated that even fairly complex x-coupled filters can be made in just one iteration. The methods are validated through measurements on manufactured coaxial cavity filters. It is also demonstrated how coupling matrix synthesis may be used to better understand and explain differences between calculated and measured filter responses.

2. Coupling

To design microwave filters a basic understanding of coupling and coupling mechanisms is necessary. In this section, the coupling mechanisms in bandpass filters are investigated and it is shown how coupling coefficients can be measured.

2.1 Inter resonator coupling

To demonstrate the concept of coupling between adjacent resonators the 2-pole circuit in ***Figure 1*** is used. Two metallic resonators are enclosed in a metallic housing and loosely coupled to the in- and output ports. The corresponding measured transmission characteristic (S_{21}) is also shown.

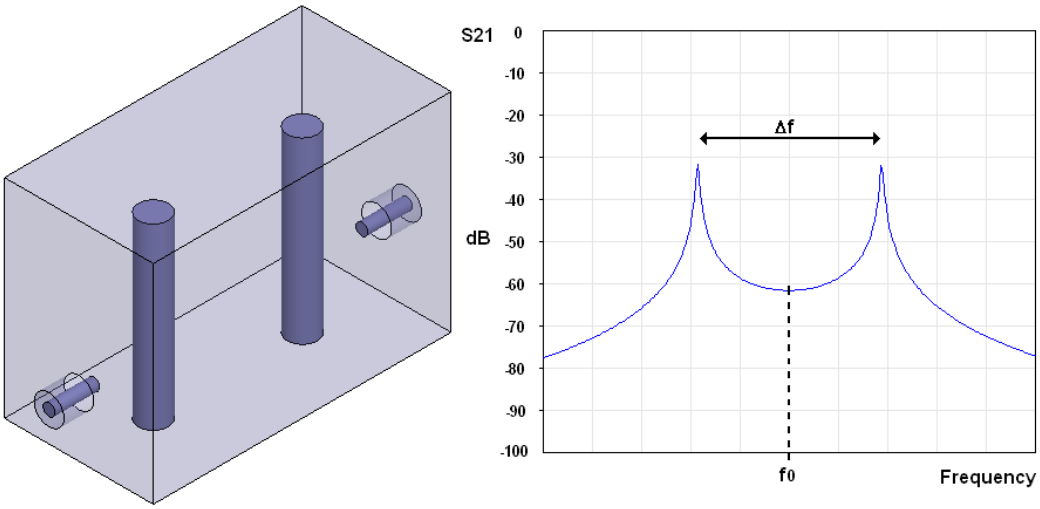

Figure 1. 2-pole box and associated transmission characteristic.

The two resonators are identical and are both resonating at frequency f_0. The coupling between the resonators results in a displacement Δf of the resonance frequencies. In this case, the coupling is Δf MHz and is referred to as the coupling bandwidth. If the coupling bandwidth is divided by the ripple bandwidth BW of the filter, we get the normalized coupling coefficient. We therefore have:

Normalized coupling coefficient: $M_{12} = \Delta f/BW$ Eq. 1

Where Δf is the coupling bandwidth, which in Hz, and M_{12} is the normalized coupling coefficient between resonator 1 and 2. To minimize the influence of in- and output connections on the coupling measurement, the resonators must be loosely connected to the input and output ports. If the top-point of the two peaks – or alternatively the "valley" between them - is kept below approximately -30 dB, the influence of the I/O ports can be neglected.

2.2 External coupling

The couplings, which connect the filter to the outside world are called external couplings and are often expressed as Q values – that is external Q's. The external Q concept can be explained by the single resonator circuit shown in ***Figure 2***. Here, the resonator is coupled to the I/O port by a rod (tapped input) but could also be coupled by, for instance, a non touching capacitive disc, a loop or similar arrangement.

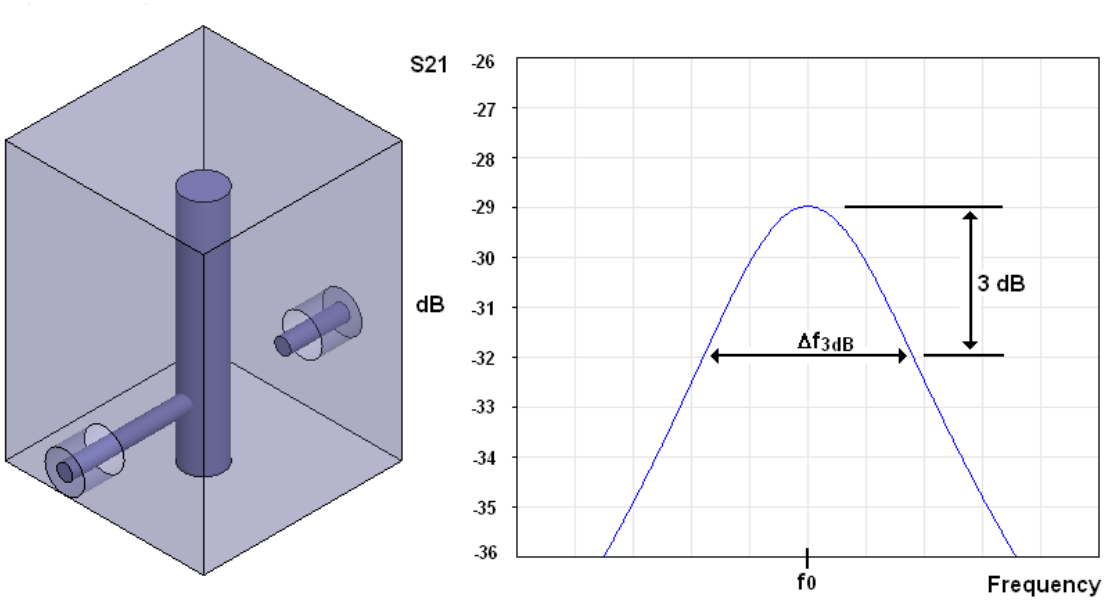

Figure 2. 1-pole box with tapped input and associated characteristic

Also shown in figure 2 is a loosely coupled "sniffer" port, which allows us to do the transmission measurement shown to the right in the figure. The influence of the sniffer port can be neglected if the peak of the resonance characteristic is kept below 25 to 30 dB.

The external coupling is found by measuring the 3 dB bandwidth of the resonance curve - denoted Δf_{3dB}. The external Q is then found by

$$Q_{ext} = Q_{loaded} = f_0 / \Delta f_{3dB} \qquad \text{Eq. 2}$$

Where it is assumed that the unloaded Q is much bigger than loaded Q so that $Q_{ext} = Q_{loaded}$ applies. Alternatively, the external Q can also be expressed by the normalized coupling coefficient M_{01}:

$$Q_{ext} = f_0 / (BW * M_{01}^2) \qquad \text{Eq. 3}$$

Where BW is the ripple bandwidth of the filter.

It is seen that a low external Q value corresponds to a wide 3dB bandwidth and hence a strong coupling. For the tapped resonator in figure 2, the coupling increases by moving the tap-point closer to the top of the resonator. It is also possible to determine the external Q by measuring the group delay of S_{11} [4].

2.3 Cross-coupling

It is well known that couplings between non-adjacent resonators - x-couplings - may be used either to:

1. introduce transmission zeroes in the stopband for increased skirt selectivity or

2. equalize the group delay in the passband

Couplings may either be inductive or capacitive and are often schematically represented as shown in ***Figure 3***. In the schematic circuit diagram, the numbered black dots represent resonators and the white circles represent source/load terminals (such as "connectors"). Inductive couplings are indicated by unbroken lines and capacitive couplings by a capacitor symbol. By convention inductive couplings are positive and capacitive couplings negative.

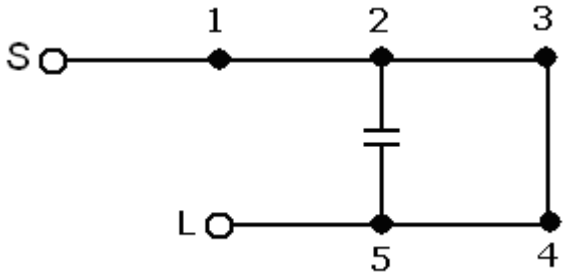

Figure 3. A 5 pole filter topology with positive main couplings and negative x-coupling.

A single x-coupling, bypassing one resonator (also called a triplet) may, under certain conditions, give rejection corresponding to approximately two extra filter poles. The use of x-couplings could in such case reduce the required filter order by two, leading to a more compact filter, which at the same time may also have lower insertion loss. The penalty is that the increased selectivity gained at one side of the passband is sacrificed by reduced selectivity on the other side of the passband. Three commonly used x-coupling configurations are shown in ***Figure 4***. These are x-couplings bypassing either a single - or two resonators.

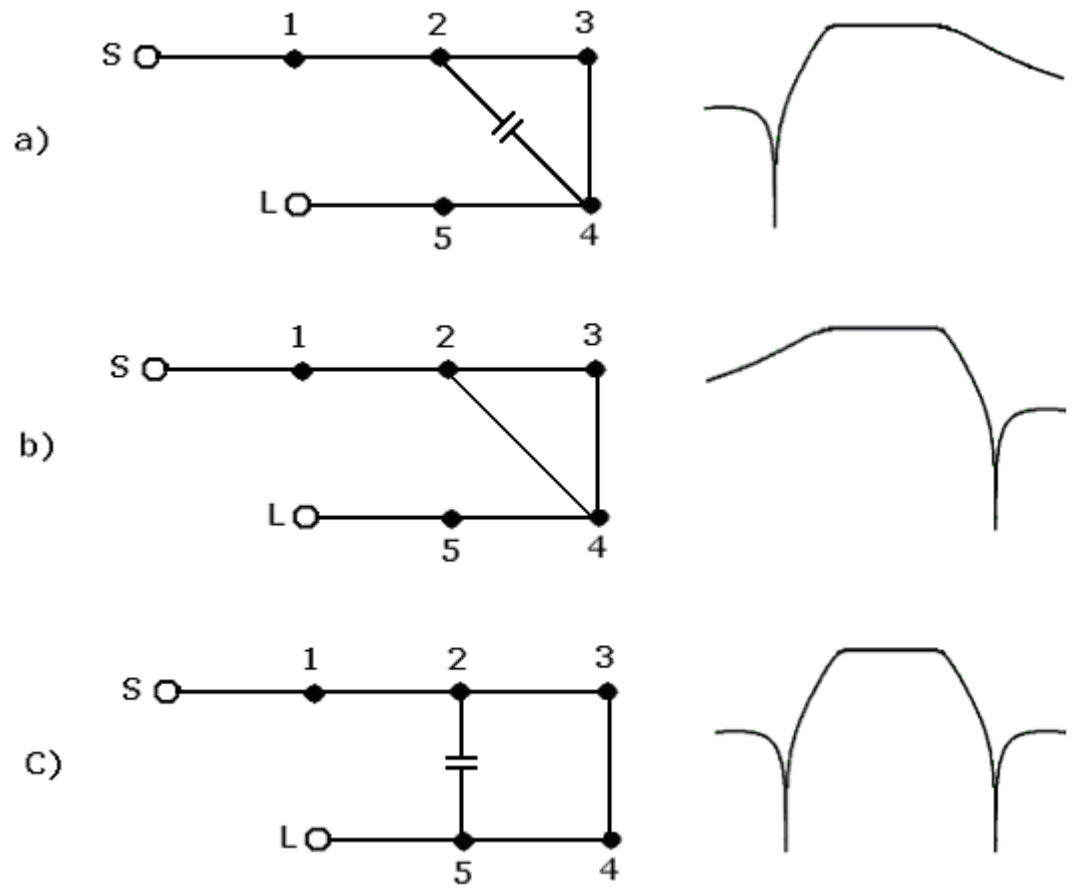

Figure 4. Three commonly used x-coupling configurations and their characteristics.
a) Triplet with negative (capacitive) x-cp
b) Triplet with positive (inductive) x-cp
c) Quadruplet with negative (capacitive) x-cp

The theory of cross-couplings is explained in the literature [6, 7] by equivalent lumped circuits and phase relationships.

2.4 Unloaded Q

The unloaded Q is not directly related to couplings but is included here because it is measured in a very similar way as the external Q. The unloaded Q is an important parameter since it is directly related to the losses of the resonator/filter and is a function of geometry as well as the materials used. If the tapped input in figure 2 is replaced by yet another loosely coupled "sniffer" port - the unloaded Q would be found instead of external Q. To estimate the unloaded Q for a circular coaxial resonator the following expression may be used:

$$Qu = \frac{0.75*n*\lambda*\mathrm{sqrt}(\pi*f0*4\pi*10^{-7}*\sigma)}{[4+n*\lambda/D2*(1+D2/D1)/\ln(D2/D1)]} \qquad \text{Eq. 4}$$

Where,

f0 = resonance frequency

σ = the conductivity of the metal forming cavity and resonator (silver: 63×10^7 Siemens/m)

D2 = cavity diameter. For rectangular cavities D2 is diameter in a circle, which has the same area as the rectangular cavity base area.

D1 = resonator diameter

λ = wavelength at f0

$n = h/(\lambda/4)$ resonator length expressed in quarter wavelengths.

h = resonator height

The factor of 0.75 is an estimate for imperfections, such as the slightly poorer conductivity that will be found in the 'real world', surface roughness, influence of tuning screws etc.

Equation 4 is a modified version of an expression [8] given for optimal unloaded Q of coaxial resonators. The original expression assumes resonator lengths, which are an integer number of a quarter wavelength ("n" is an integer). The formula is, however, found to be useable also for other resonator lengths and, in Equation 4, "n" is a real number (such as 0.5 for a $\lambda/8$ resonator). Microwave filters may be implemented in many different ways. Very often it is the loss requirement, which dictates the filter technology that must be used. Some indications of typical unloaded Q's for different resonator types are given in **Table 1**.

Technology	**Unloaded Q**
Microstrip, stripline & coplanar	100 - 600
Coaxial cavity & combline	1000 - 6000
Waveguide	4000 - 15000
Dielectric resonator	5000 - 50000

Table 1. Different resonator types and corresponding unloaded Q's

3. Coupling Matrix Synthesis

A lowpass prototype filter can be described by a normalized coupling matrix **M** of order N+2, where N is the filter order [5]. The term "lowpass prototype" refers to that it is centred around 0 (zero) rad/s and has upper and lower corner frequencies of +/-1 rad/s. Once a prototype network has been synthesized, a frequency transformation is applied, which transforms the lowpass prototype to a bandpass filter with the right centre frequency and bandwidth.

Synthesis of lowpass prototype networks - and hence filter characteristics and coupling matrices - is well described in the literature [2, 3, 5] and will not be dealt with here. In the following, Guided Wave Technology's Filter and Coupling Matrix Synthesis tool (CMS) [9] is used for this purpose.

3.1. The N+2 Coupling Matrix

The N+2 normalized coupling matrix **M** is a full description of all coupling paths in a filter. The order of **M** is N+2, where N is the filter order. **M** is a symmetric matrix with real elements M_{ij}. The '+2' term refers to that the N+2 coupling matrix is extended to include also the input and output connections. ***Figure 5*** explains the N+2 coupling matrix in more detail for the folded topology.

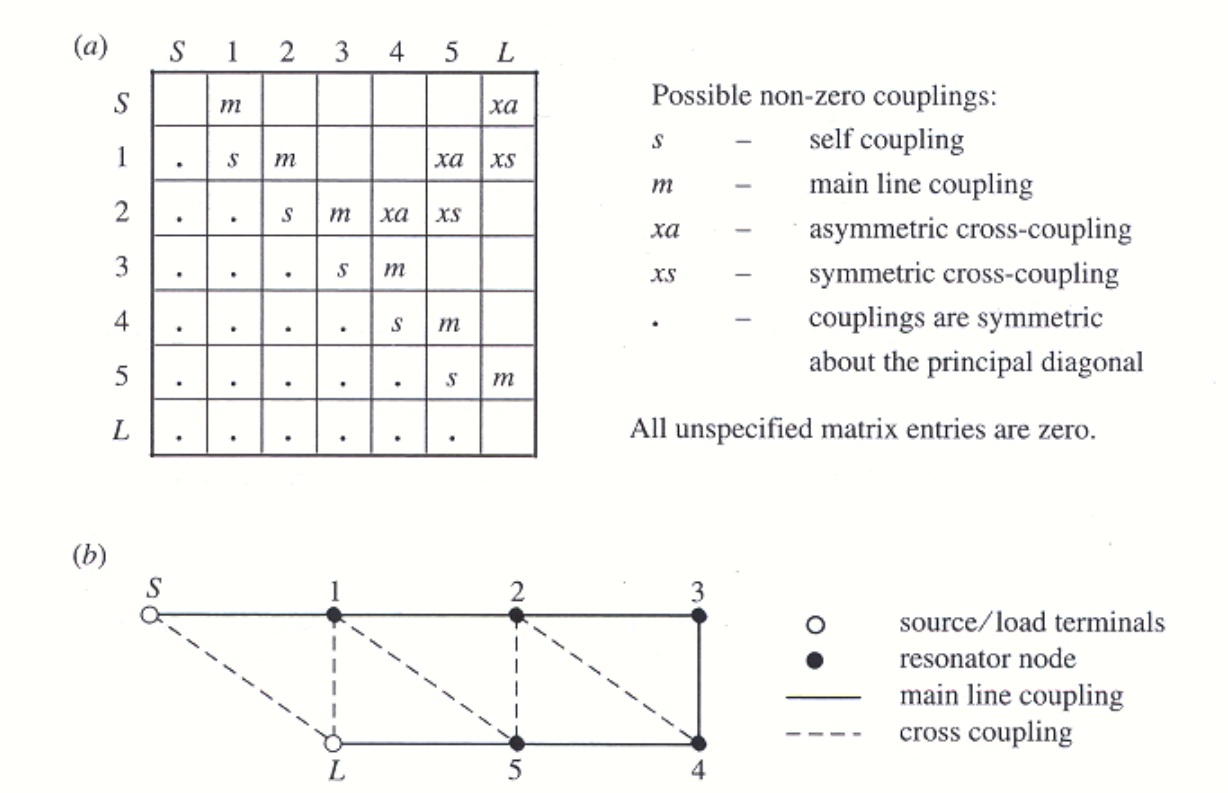

Figure 5. Folded network coupling matrix form - fifth degree example.
(a) Folded coupling matrix form. "s" and "xa" couplings are zero for symmetric characteristics. (b) Coupling and routing schematic. Figure reprinted from [2].

The N+2 coupling matrix includes the input/output couplings in the synthesis. Couplings may therefore be made directly from the source/load nodes to internal resonators – or directly between the source and load. Fully canonical filtering functions (that is Nth-degree characteristics with N finite-position transmission zeroes) may also be synthesized. The self couplings "s" in the main diagonal in figure 5 represent the resonance frequencies of the individual resonators. In an x-coupled filter the bypassed resonators will have frequencies which deviate

from the center frequency - f_0 - of the filter. In a filter without x-couplings, the main diagonal elements will all be 0 (meaning that all resonators are tuned to f_0).

Outside the main diagonal, the normalized couplings - M_{ij} - may be transformed to coupling bandwidths by multiplying by the ripple bandwidth. Coupling matrix synthesis gives results which are fully equivalent to filters realized by lumped element (that is RLC) theory. Filters synthesized and analyzed in this way do therefore not account for effects related to the use of transmission lines as resonating elements or couplings. Couplings are assumed frequency invariant and the results obtained by coupling matrix synthesis are therefore most accurate for narrow band filters (relative BW < 10%) in - and close around - the passband.

4. Filter Design Example 1

The best way to demonstrate filter and coupling matrix synthesis is through an example. A coaxial cavity WiMAX filter was designed and built.

The filter has the following specifications:

Center frequency:	f0 = 3440 MHz
Ripple bandwidth**:**	BW = 70 MHz
Rejection:	>50 dB @ f0+/- 80 MHz
Returnloss:	RL > 20 dB (3405 MHz to 3475 MHz)
Insertion loss:	IL < 1.0 dB
Ripple:	< 0.5 dB
Temperature range**:**	-30 to +70 ºC
Power handling:	< 20 dBm
Connectors:	SMA female
Connector positions**:**	In- and output connections must be in the same end of the filter
Material:	Silver plated Aluminium
Mechanical dimensions:	No requirements

Comments to the specifications:

- The relative bandwidth of this filter is 2 percent, which is sufficiently narrowband so that coupling matrix synthesis methods may be used with good accuracy.

- 20 dB return loss corresponds to $|S_{21}|$ = -0.04 dB. The ripple bandwidth is the frequency band between the two outermost -0.04 dB points in the S_{21} characteristic (like 3 dB bandwidth is between the 3 dB points).

- The rejection requirements are symmetrical about the center frequency.

- The temperature range is 20 ºC +/- 50 º. In this temperature range, the filter center frequency will drift several MHz depending on resonator material. In the present case a +/- 5 MHz temperature allowance is assumed for a start.

The design bandwidth is therefore increased from 10 to 80 MHz. At room temperature, all specifications should therefore be met with this extended bandwidth

- Power-handling. The filter needs only be able to withstand 20 dBm (0.1 W) of RF power. No special precautions to avoid arcing in the filter need therefore to be taken. In Tx filters arcing may be a big problem, for instance if not sufficient space exists between resonators and tuning screws [10].

- Connector placement in the same side of the filter calls for a folded topology.

4.1. Synthesis of Filter Characteristics

With the above comments in mind, the first task is to determine the needed filter order N and to decide on the use of transmission zeroes. For this purpose the CMS tool [9] is used. A screen dump of the synthesized filter characteristics is shown in ***Figure 6***. The characteristic shown is found in a few trials. Since there are symmetrical rejection specifications on both sides of the passband, it is natural with two symmetrically placed transmission zeroes. With such two transmission zeroes, it is found that a 6th order filter will give approximately 55 dB rejection in the stopband. This gives a 5 dB margin to the specifications, which seems reasonable.

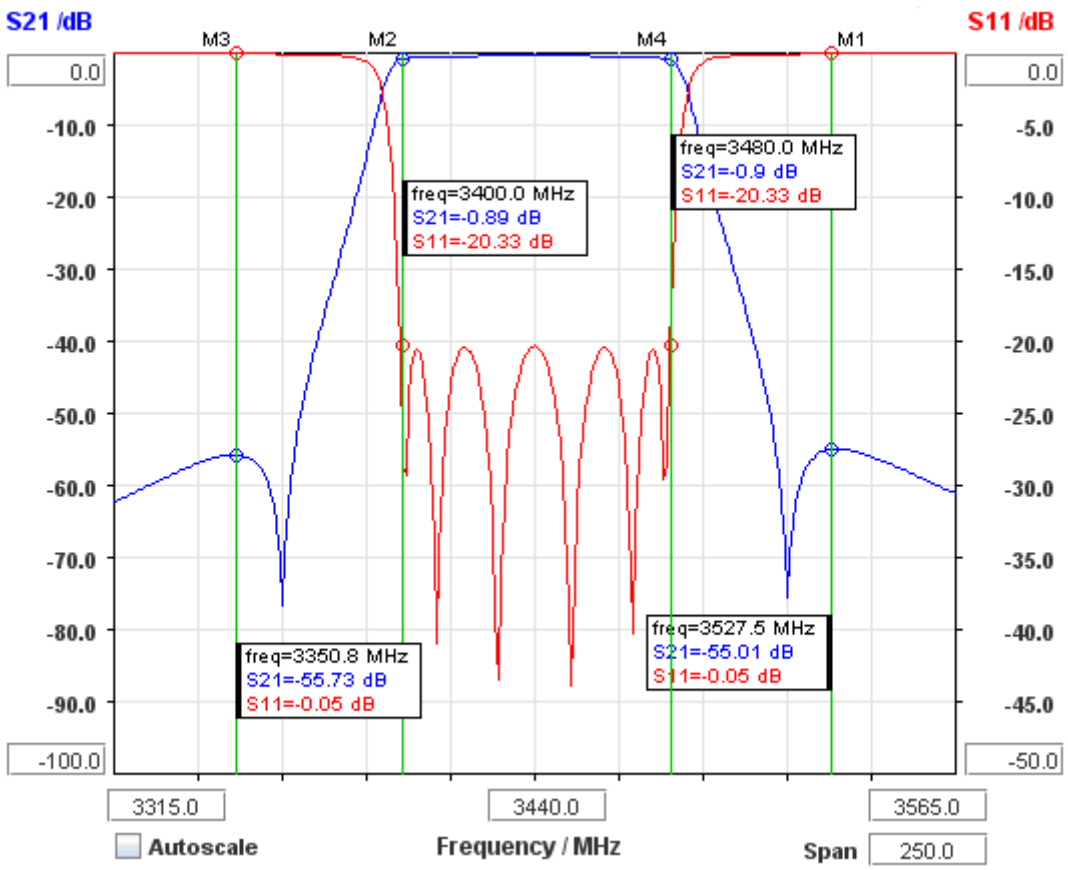

Figure 6. CMS generated filter characteristics. Filter order N = 6. Ripple BW = 80 MHz. Unloaded Q = 4000. Transmission zeros placed symmetrically at f0 +/- 75 MHz. The vertical marker lines sample the filter performance at critical points.

Without transmission zeroes, a 7th order filter would be necessary. The extra cavity in this case would lead to a filter with increased dimensions – and losses. The 6th order design with two symmetrical placed transmission zeroes, shown in figure 6, therefore seems a good compromise. The transmission zeroes in figure 6 have been placed at f0 +/- 75 MHz.

4.2. Determination of Cavity Dimensions

The required unloaded Q is an input parameter, which may be varied in CMS until the insertion loss at the band edges meets the specification with some margin. In the present case, an unloaded Q of 4000 gives a 0.9 dB insertion loss, which is 0.1 dB better than specifications. Some margin is necessary to compensate for excess losses originating from brass tuning and coupling screws, cross coupling rods and connector losses, for instance.

The next task is to determine the resonator length. If too long resonators are chosen, the filter passband will come out too low in frequency and cannot be tuned up to the right frequency, since the insertion of tuning screws moves the passband

further down in frequency. The right length may be found experimentally in a few trials or by use of a 3D EM simulator like HFSS. Without tuning screw, the right resonator length must give a resonance frequency above the wanted f_0 of the filter. Insertion of the tuning screw will bring the frequency down to the right value. In this way the resonance frequency may be tuned in at values both above and below f_0. As a rule of thumb the resonator length should be between 50 and 80 percent of a quarter wavelength. In the present case we chose:

Lres = 12 mm (55 percent of λ/4)

Once the unloaded Q and resonator length have been determined, it is time to calculate the coaxial cavity dimensions.

From Equation 4, it is found that a circular silver-plated cavity with diameter 40 mm and resonator diameter 10 mm will give an unloaded Q of approximately 4000. The corresponding square cavity will have a side length 35 mm.

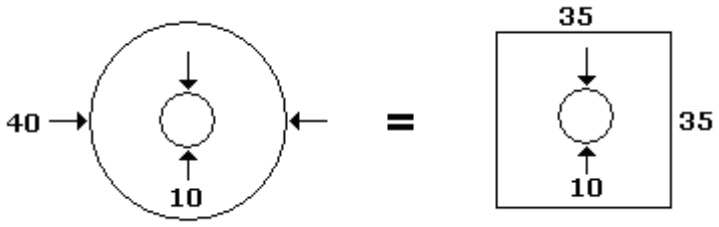

Figure 7. Two different cavity types with approximately same base area and unloaded Q's.

The optimal ratio between inner- and outer diameters in a circular coaxial cavity is close to 1:3.6 for highest unloaded Q. The unloaded Q varies, however, slowly with this ratio and resonator diameters between 9 and 14 mm give almost identical results in a circular cavity with 40 mm diameter. The height of the cavity is fixed at 20 mm, which gives an 8 mm tuning screw headroom from resonator top to cavity lid. Finally a square resonator geometry is chosen. The dimensions are summarized in ***Figure 8***.

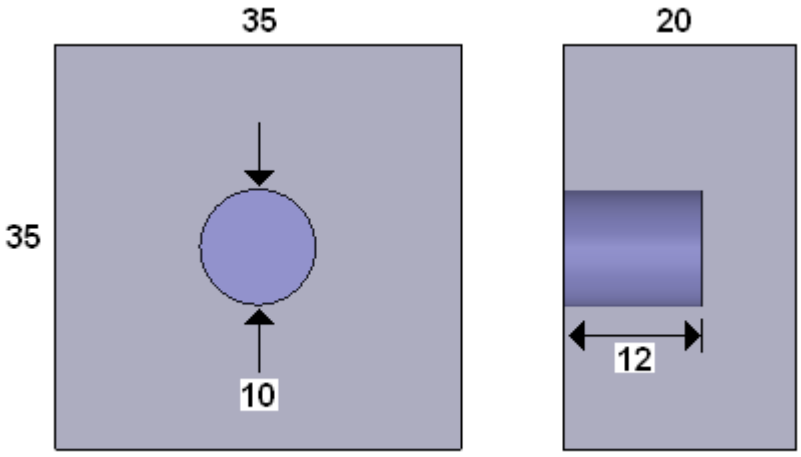

Figure 8. Final resonator geometry for WiMAX filter

4.3 Determination of Coupling Dimensions

Once the cavity geometry has been fixed, the coupling geometry may be determined. It was previously determined that a folded 6-pole topology will meet the specifications. With help from the CMS tool, it is found that the characteristic shown in figure 6 may be realized by the topology and coupling matrix shown in ***Figure 9***.

a)

	S	1	2	3	4	5	6	L
S	0	0.9986	0	0	0	0	0	0
1	0.9986	0	0.8365	0	0	0	0	0
2	0	0.8365	0	0.5997	0	-0.0744	0	0
3	0	0	0.5997	0	0.642	0	0	0
4	0	0	0	0.642	0	0.5997	0	0
5	0	0	-0.0744	0	0.5997	0	0.8365	0
6	0	0	0	0	0	0.8365	0	0.9986
L	0	0	0	0	0	0	0.9986	0

b)

	S	1	2	3	4	5	6	L
S	3440	79.9	0	0	0	0	0	0
1	79.9	3440	66.9	0	0	0	0	0
2	0	66.9	3440	48	0	-6	0	0
3	0	0	48	3440	51.4	0	0	0
4	0	0	0	51.4	3440	48	0	0
5	0	0	-6	0	48	3440	66.9	0
6	0	0	0	0	0	66.9	3440	79.9
L	0	0	0	0	0	0	79.9	3440

c)

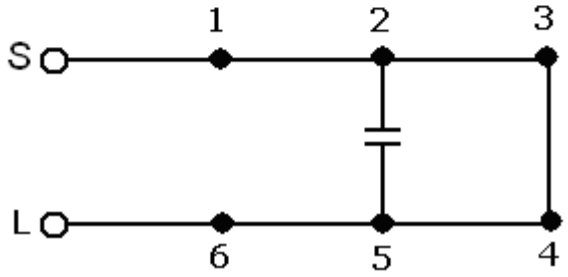

Figure 9. Folded coupling matrix and topology realizing the filter characteristic shown in figure 6. The couplings are displayed in different ways: a) Normalized coupling coefficients, b) Coupling bandwidths, c) Topology

It is noted that the x-coupling between resonators 2 and 5 is negative (that is capacitive) and is much weaker than the mainline couplings. It is also seen that since the characteristic is symmetric, the x-coupling has not had any effect on the resonance frequencies of the resonators, since they are all at 3440 MHz. Asymmetric x-couplings would have detuned some of the resonators. The strongest coupling is between the source/load terminals and the first/last resonator (that is the external couplings). The external coupling bandwidth (79.9 MHz) is almost identical to the ripple bandwidth of the filter (80 MHz), and the main line coupling bandwidths have values between 48 MHz and 66.9 MHz. The x-coupling is 6 MHz. In the following the dimensions of main line coupling apertures will be determined.

4.3.1. Determination of Main Line Coupling Aperture Dimensions

The procedure used here to find the coupling aperture dimensions will be referred to as the "2-pole box" method, and may either be carried out by use of a 3D

simulator or experimentally. The procedure is to construct a 2-pole box as explained in section 2.1. (and shown in figure 1) and vary either the distance - or the aperture opening - between the two resonators and at the same time monitor the resulting coupling bandwidths. In this way, a curve can be made, which shows the relationship between coupling bandwidth and for instance the aperture dimensions. It is clear that this is done most easily in a 3D simulator like HFSS [11] or CST [12], but if such tools are not available, the 2-pole box may be constructed physically and the coupling bandwidths measured on a network analyzer.

If a 3D simulator is available, a more advanced technique may also be used, in which the coupling between more than just two neighbouring resonators is taken into account. This technique is called co-simulation [13], and combines 3D modelling and circuit simulation techniques. In the present article, however, the simpler 2-pole box method will be demonstrated and it is shown that, with this method, it is possible to get good results in only one iteration.

With the resonator/cavity as defined in figure 8, a 2-pole box is constructed as shown in ***Figure 10***. Instead of the HFSS model shown here, a similar aluminium prototype may also be manufactured.

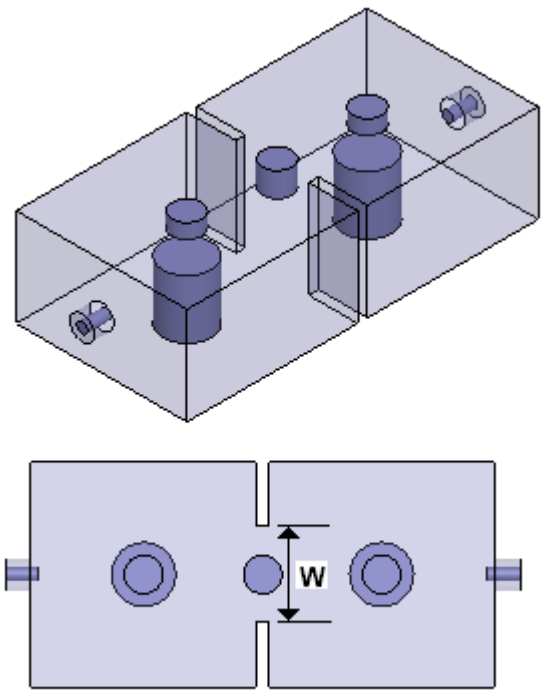

Figure 10. 2-pole coupling box for the 3.44 GHz WiMAX filter.

The 2-pole box in figure 10 has two 6 mm tuning screws placed in the lid above the resonators and one 6 mm coupling screw placed in the middle of the aperture opening in the lid. The coupling screw allows tuning of the coupling: The

longer the coupling screw goes into the aperture the stronger the positive (inductive) coupling becomes [6]. The coupling screws are included in the HFSS model in order to be able to increase or decrease the coupling bandwidth in the final filter. The lengths of the tuning screws are adjusted (and must always have equal lengths) until the two resonance tops are placed symmetrically around f_0 = 3.44 GHz as shown in figure 1. The coupling bandwidth for this aperture width is then the distance between the two resonance peaks. The thickness of the wall between the two cavities is 2 mm.

If a 2-pole box is manufactured physically, the procedure for tuning in to f_0 and measuring the coupling on a network analyzer is as follows:

- First one of the tuning screws is screwed in until it short circuits with the top of the resonator.
- Then the other tuning screw is adjusted until the single resonance peak is positioned at f_0 = 3.44 GHz.
- Finally the shorted screw is released until the – now two – resonance peaks are placed symmetrically around f_0 = 3.44 GHz as shown in figure 1.
- The coupling bandwidth for this aperture width is then the distance between the two resonance peaks.

Instead of manufacturing several 2-pole boxes with different aperture widths, a single one may suffice if the opening is gradually widened up and the coupling bandwidths are measured along in the process.

With both methods, the obtained coupling will only be accurate if the resonance tops are kept below approximately -30 dB.

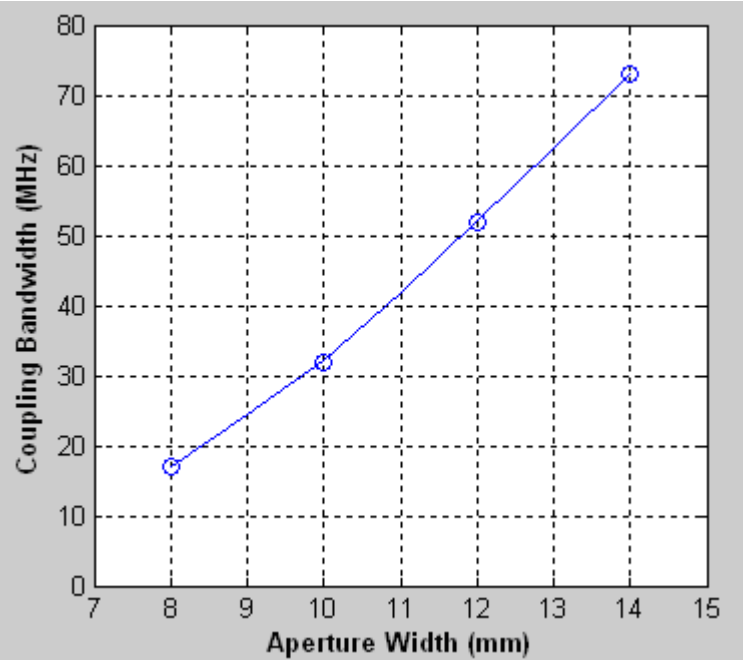

Figure 11. HFSS simulated couplings. The blue circles represent the four simulated apertures

Figure 11 shows the result of the coupling simulation on the HFSS model in figure 10.
The coupling bandwidths for aperture widths: 8, 10, 12 and 14 mm have been calculated and are marked with circles in the plot. A curve has been fitted to the four points.

From this curve, it is now possible to find the aperture openings, which correspond to the wanted main line coupling bandwidths as shown in figure 9b. The result is listed in **Table 2.**

Resonator from / to	Coupling BW MHz	Aperture Width mm
1 / 2	66.9	13.4
2 / 3	48.0	11.6
3 / 4	51.4	15.4
4 / 5	48.0	11.6
5 / 6	66.9	13.4

Table 2 Mainline coupling aperture dimensions

The coupling between resonator 3 and 4 is not found from figure 11, since the wall thickness between these two cavities is 5 mm – and not 2 mm as between the other cavities. This increased thickness is necessary in order to be able to cut threads for the lid in the centre wall (see ***Figure 12***).

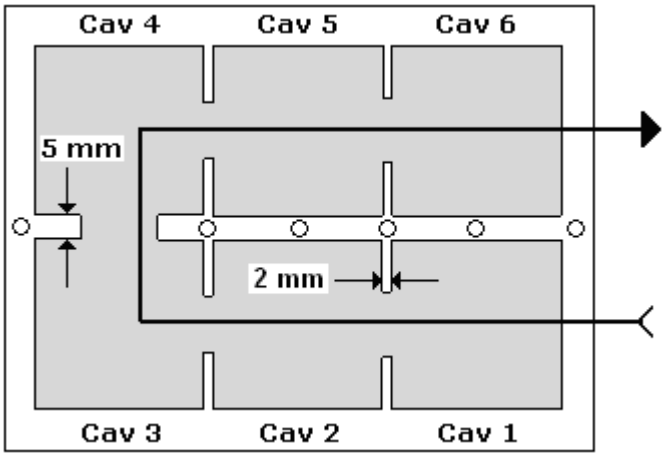

Figure 12. Filter outline showing thread holes in the centre wall

The aperture width between cavities 3 & 4 has been found by a separate 2-pole box simulation.

4.3.2. Determination of X-coupling Dimensions

According to figure 9b, a negative (that is capacitive) 6 MHz x-coupling is needed between cavity 2 & 5. Coaxial resonators at resonance have high voltages (hence strong electric-fields) near the resonator top and high current density (hence strong magnetic fields) near the bottom. Two such resonators therefore couples capacitively in the top region and magnetically at the bottom region. In the present case negative coupling may therefore be implemented by an opening in the upper part of the wall, which will allow the electric fields to interact. To "amplify" the capacitive coupling a metallic rod may be suspended in the opening between the resonators. The length of this rod determines the strength of the coupling. The 2-pole box model for measuring the capacitive x-coupling is shown in ***Figure 13***. In practice the metallic rod is fixed by a PTFE plug or similar dielectric material.

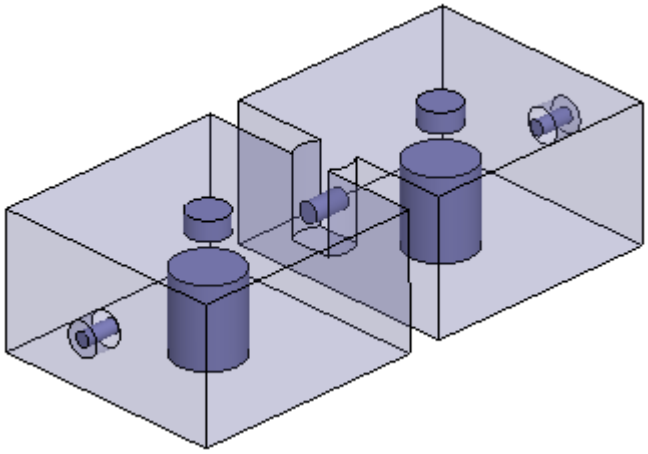

Figure 13. Implementation of negative coupling by a suspended metallic rod (3 mm diameter x 5.5 mm) in the aperture between the cavities.

HFSS simulations on the 2-pole box with such small couplings are normally not very accurate. One must therefore be prepared to find the right rod length experimentally once the filter has been manufactured

4.3.3. Determination of I/O Couplings.

The final coupling, which needs to be determined in the filter, is the coupling between the I/O connectors and the first/last resonator in the filter. This coupling will be of the type in figure 2, where the centre conductor of the SMA connector is soldered to the resonator ("tapped"), at a certain height above the ground plane. The corresponding 1-pole box for determining this height is shown in ***Figure 14***. The weakly coupled port to the right allows a transmission measurement.

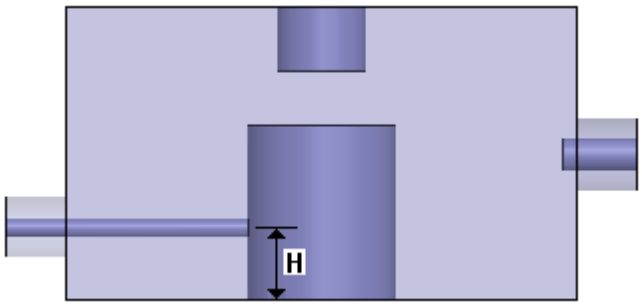

Figure 14. HFSS 1-pole box model for determining the tap height 'H'.

The external Q found from the 1-pole box "measurement" is related to the external normalized coupling coefficient M01 as described by Eq. 3. An external Q is desired which corresponds to a M01 equal to 0.9986 or 79.9 MHz (figure 9).

The HFSS calculated dependency between external coupling bandwidth and tap height is shown in ***Figure 15***.

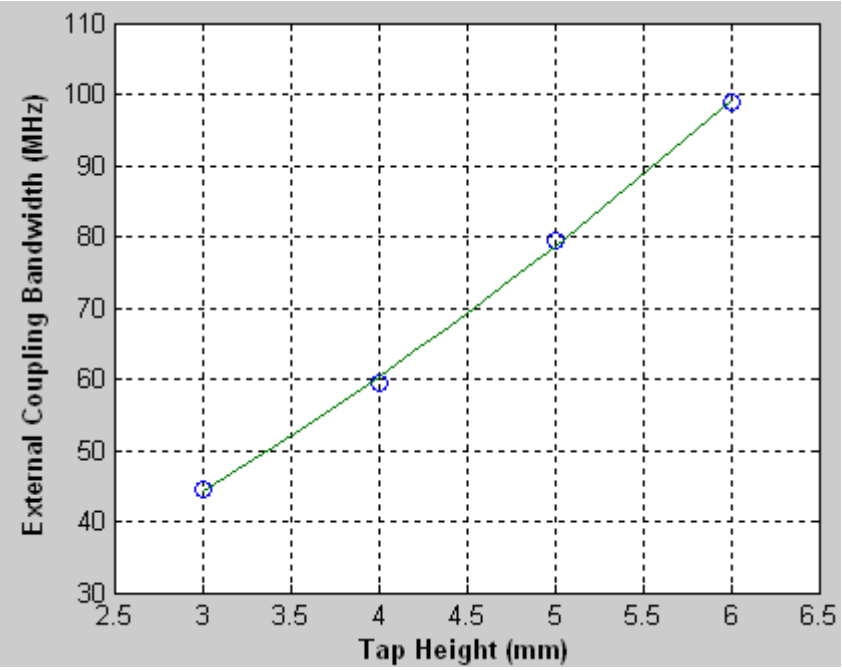

Figure 15. HFSS simulated external couplings vs. tap-height. The wanted external coupling bandwidth (79.9 MHz) is achieved with a tap-height of 5.0 mm

4.4. Design Review for Filter Design Example 1

All filter dimensions have now been determined and the filter can be manufactured.
The design flow for this filter is summarized below.

Desired filter property	**Found from**
Filter order & transmission zeroes	Stopband rejection
Unloaded Q	Insertion Loss Requirement
CMS synthesis of filter characteristics	
Topology	Connector positions & transmission zeroes
Resonator length	Centre frequency fo
Cavity dim. & resonator diameter	Unloaded Q
CMS determination of coupling coefficients	
Main line aperture dimensions	Coupling Matrix + 2-pole box
X-coupling dimensions	Coupling Matrix + 2-pole box
Tap height on I/O resonators	Coupling Matrix + 1-pole box

Table 3. Overview of filter properties and driving parameters

4.5. Prototype Evaluation - Design Example 1

A filter with dimensions as found in the previous sections has been manufactured. The resonators have been manufactured separately so that adjustments can be made to the lengths - should it become necessary. The resonators are therefore mounted in the filter body with screws. Resonators, filter body and lid are silver plated (3 – 5 micron). A picture of the filter is shown in ***Figure 16***.

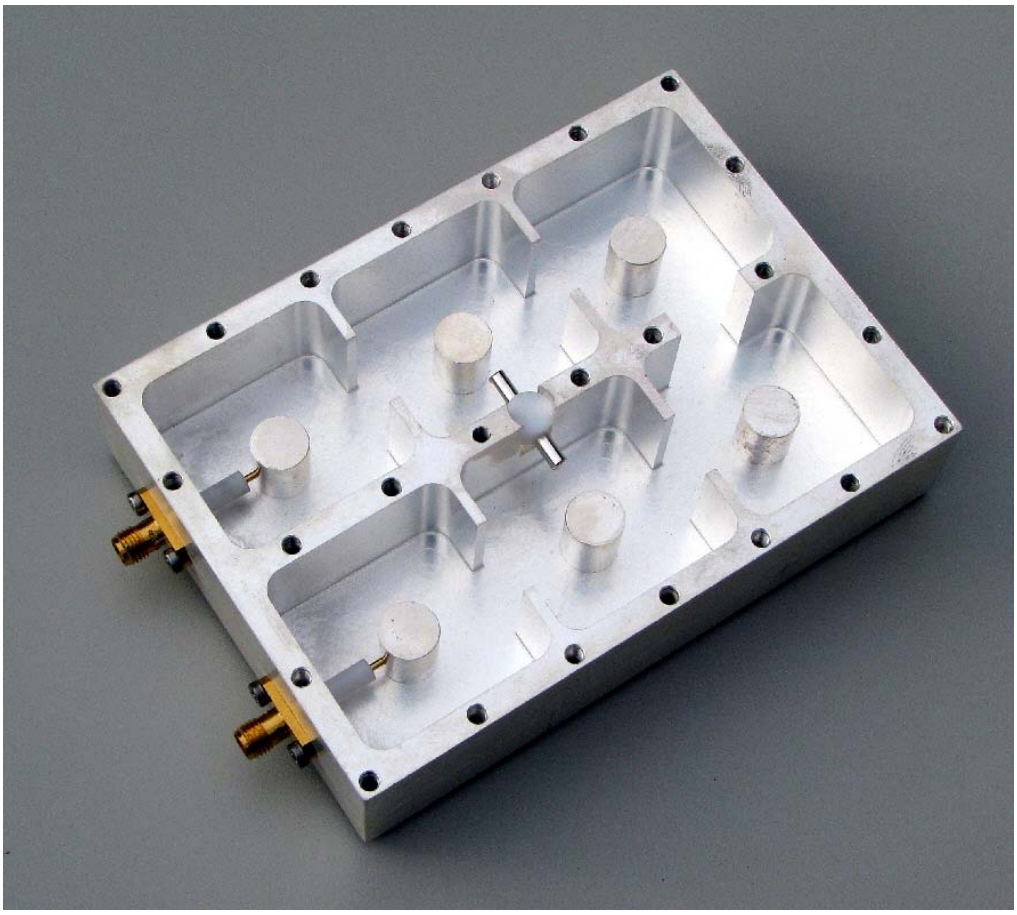

Figure 16. Photograph of the manufactured WIMAX filter

The filter was tuned without any mechanical modifications of apertures and resonator lengths. The only component which needed a touch was the x-coupling rod which had to be increased in length compared to what was found from HFSS.

The measured characteristics are shown in ***Figure 17***. Compared to the synthesized characteristic in figure 6, it is seen that very good agreement exists, although the two transmission zeroes are not strictly symmetrically positioned about the centre frequency in the manufactured filter.

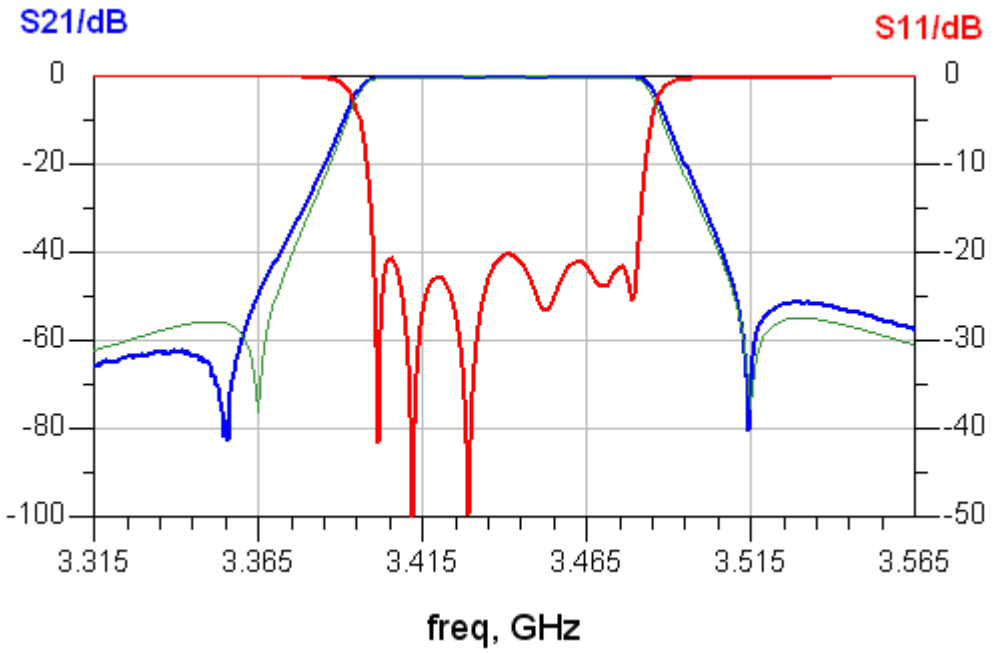

Figure 17. Measured S-parameters (thick curves) of manufactured filter.
Also shown as reference is the synthesized S21 characteristic (thin green line)

A summary of specifications and obtained results is shown in **Table 4**.

Parameter	Freq Range	Requirement	Obtained
Insertion loss	f = 3400 MHz	1 dB	0.79 dB
	f = 3480 MHz	1 dB	0.68 dB
Ripple	3400 MHz to 3480 MHz	0.5 dB	0.39 dB
Return Loss	3400 MHz to 3480 MHz	20 dB	20 dB
Rejection	f < 3360 MHz	50 dB	62.1 dB
	f > 3520 MHz	50 dB	51.4 dB

Table 4. Comparison between specifications and obtained results

From table 4, it is seen that all specifications are met in the manufactured filter but for the rejection above the passband, the obtained margin is smaller than expected due to the asymmetrically placed zeroes.

4.5.1. Investigation of Transmission Zero Asymmetry

This asymmetry is now investigated a little further. The notch above the passband is located correctly, but the notch below the passband is 11 MHz too low compared to the synthesized reference. In order to find out what has caused this small asymmetry, the measured characteristic shown in figure 17 has been recreated in CMS simply by displacing the left notch 11MHz down in frequency. The corresponding folded coupling matrix has then been synthesized.

The result is shown in ***Figure 18***.

	S	1	2	3	4	5	6	L
S	3440	79.9	0	0	0	0	0	0
1	79.9	3439.9	67	0	0	0	0	0
2	0	67	3439.9	48.2	0	-5.1	0	0
3	0	0	48.2	3439.5	50.5	3.1	0	0
4	0	0	0	50.5	3442.8	48.1	0	0
5	0	0	-5.1	3.1	48.1	3439.9	67	0
6	0	0	0	0	0	67	3439.9	79.9
L	0	0	0	0	0	0	79.9	3440

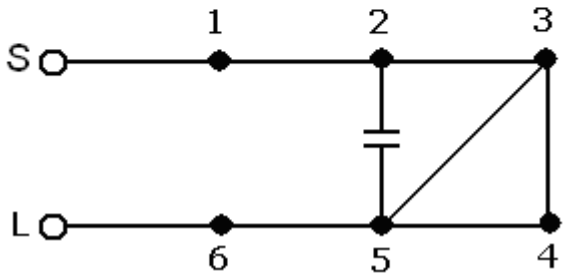

Figure 18. Coupling matrix and topology circuit duplicating the slightly asymmetric measured response in figure 17..

It is seen that the asymmetric response may be caused by unintended positive coupling between resonator 3 and 5. It is clear by inspection of the filter geometry shown in figures 12 & 16 that if stray coupling exists between resonator 3 and 5 the same coupling will also exist between resonator 2 and 4. The asymmetric characteristic is therefore the result of the combined non-adjacent couplings between the mentioned four resonators.

A possible way to reduce the asymmetry would be to improve the isolation between resonator 3 and 5 and between 2 and 4. One way of doing this could be to move the coupling apertures (see figure 12) away from the centre in the cavities and closer to the outer walls in the filter. In practice it is almost impossible to obtain 100 percent symmetric characteristics, since there will always be some unintended leakage coupling between non-adjacent resonators in the filter.

5. Filter Design Example 2

In this example the filter designed in the previous example will be modified in order to get a flat group delay in the passband. Complex transmission zeroes placed in the pass band will change the group delay characteristic of a filter. If we take the filter designed and manufactured in the previous example and introduce the complex conjugated transmission zero pair 3440 + j42 and 3440 - j42, the result shown in ***Figure*** 19 results (blue curves). Again it is not the scope of this article to

go deeper into the underlying equalization procedures. More information on how this is practically done can be found in [9].

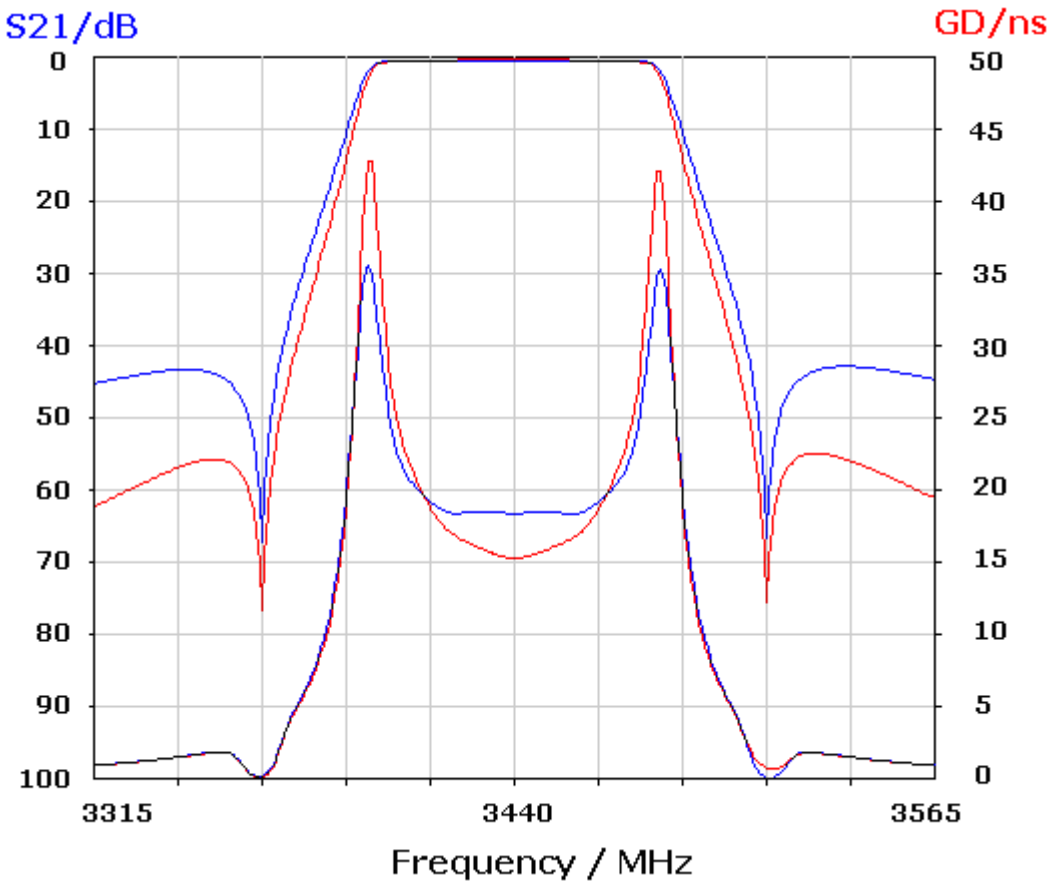

Figure 19. CMS group delay comparison. Red: Un-equalized filter. Blue: Equalized filter

The comparison in figure 19 shows that flattening of the group delay is achieved by a penalty in stop band attenuation. The coupling matrix, which yields the equalized characteristic in figure 19, is shown in ***Figure 20***. The corresponding filter is almost identical to the filter designed in the previous example (figure 6) - except for the group delay equalization. The reduced stopband attenuation in the equalized filter is simply a result of the extra x-coupling (between resonator 1 and 6), which has introduced a new and shorter path between input and output.

	S	1	2	3	4	5	6	L
S	3440	80.3	0	0	0	0	0	0
1	80.3	3440	67.6	0	0	0	-2.8	0
2	0	67.6	3440	48.9	0	5.8	0	0
3	0	0	48.9	3440	43	0	0	0
4	0	0	0	43	3440	48.9	0	0
5	0	0	5.8	0	48.9	3440	67.6	0
6	0	-2.8	0	0	0	67.6	3440	80.3
L	0	0	0	0	0	0	80.3	3440

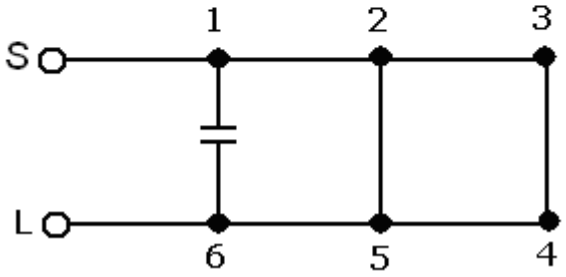

Figure 20. Coupling matrix and topology for group delay equalized WIMAX filter

Implementation of a physical filter from the coupling matrix in figure 20 follows the exact same procedure as in the previous example – in fact we can find all mainline couplings from Figure 11. The external coupling bandwidth is 80.3 MHz and hence only 0.4 MHz different from what we had in the previous example. The tap height from the previous example is therefore maintained in the present filter (that is 5.0 mm). It is also noted that the coupling between resonator 3 and 4 is reduced quite a lot compared to the previous example.

5.1. Implementation of X-couplings

Again the two x-couplings in this filter are so weak that their dimensions will be difficult to determine accurately by 2-pole box methods (or by any method). Unintended positive ("stray") coupling between the resonators will exist and will make coupling adjustments necessary in the final filter. Instead, we will prepare the filter mechanics so that these two couplings may be adjusted experimentally to the right values once the filter house is manufactured.

The positive (inductive) coupling will be implemented by a narrow opening from top to bottom in the common wall between cavities 2 and 5. This coupling will be adjusted by a screw from the lid into the aperture.

The negative (capacitive) coupling will be implemented by an opening in the top of the common wall between cavities 1 and 6 in which a capacitive rod is placed - just as described in the previous example. The length of the rod will be adjusted experimentally.

5.2. Prototype Evaluation - Design Example 2

The group delay equalized filter described in the previous sections has been manufactured. A photograph of this filter is shown in ***Figure 21***.

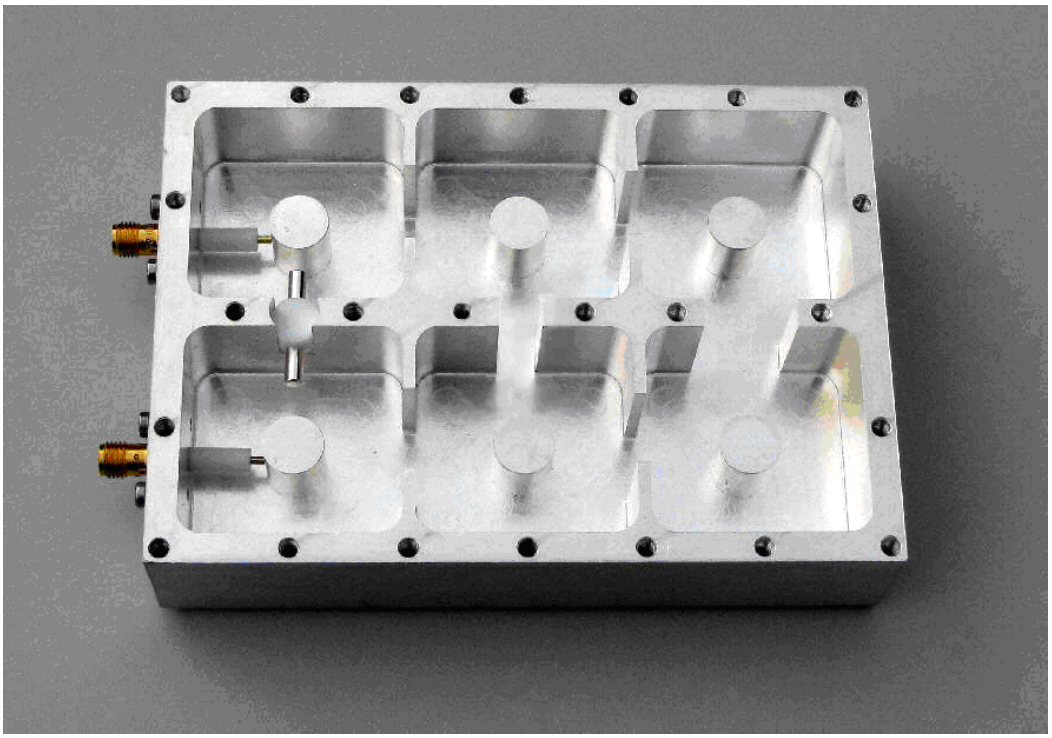

Figure 21 Manufactured equalized 6-pole WIMAX filter

Again this filter was tuned without any mechanical modifications of apertures and resonator lengths. The only component which needed mechanical adjustment was again the x-coupling rod between resonator 1 & 6 which had its length adjusted. The x-coupling between resonator 2 & 5 was adjusted by the coupling screw in the lid.

The measured result is compared with the CMS synthesized characteristics in ***Figure 22***.

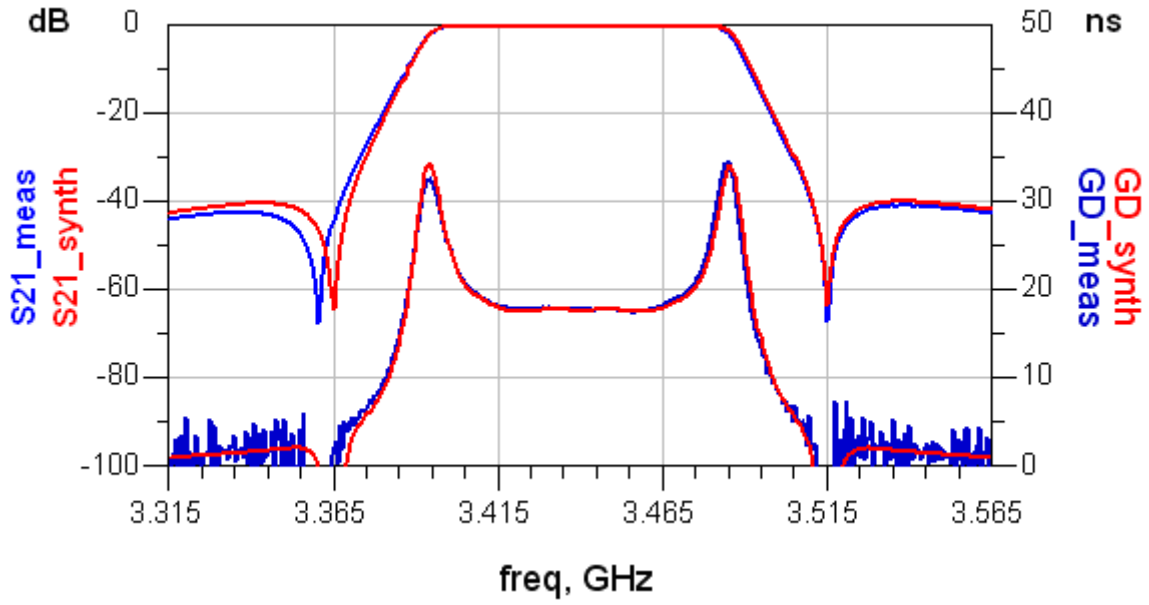

Figure 22. Comparison of group delay equalized filter characteristics.
Synthesized (red) Measured (blue)

It is seen that excellent agreement exists between the synthesized characteristics and the measured performance. Again, the transmission zeroes are slightly asymmetrically positioned since the lower zero is displaced 5 MHz down in frequency.

The asymmetrical characteristic can be entered in the CMS tool in order to find out which unintended couplings may have caused the asymmetry. If this is done, it is found that positive (inductive) coupling between resonator 2 and 6 may cause such asymmetry. At first glance it may seem strange that two such remote resonators can "see" each other (figure 21), but the x-coupling aperture in the wall between resonator 2 and 5 may also at the same time serve as at shortcut for positive coupling between resonator 2 and 6.

6. Conclusion

This article has dealt with the practical aspects of making physical microwave bandpass filters based on coupling matrix synthesis. With the coupling matrix synthesis approach, a set of filter S-parameter characteristics is first created by proper choice of filter order, return loss, unloaded Q and position plus number of transmission zeroes. Then a suitable filter topology is defined and finally the corresponding coupling matrix is synthesized.

This coupling matrix fully defines the filter and, with this at hand, the corresponding physical filter can be designed and manufactured. To close the gap between the coupling matrix representation of a filter and the physical filter, practical directions about how to measure/calculate coupling bandwidths and external Q are given. These parameters can be determined either by use of 3D EM

simulators or by measurements, and procedures have been given for both by use of the “2-pole box” method.

To demonstrate the design process, two 6th order coaxial cavity filters for WIMAX applications at 3.44 MHz have been synthesized using the coupling matrix synthesis method and then manufactured. The first filter has been synthesized as a folded topology with two symmetrically positioned transmission zeroes about the centre frequency. A single negative x-coupling has been applied to get the wanted characteristic. Dimensions of cavities, resonators, coupling apertures and I/O tap heights have been determined and the filter has been manufactured. Measurements on the manufactured filter have shown excellent agreement with the synthesized characteristics.

The second – and more advanced filter example – is almost identical to the first filter – but group delay flattening has furthermore been introduced in the passband, by placing a pair of complex transmission zeroes at the centre frequency. The wanted characteristic has been obtained by introducing a negative and a positive x-coupling in the filter. Measurements on this filter have again shown excellent agreement with the synthesized characteristics.

The conclusion of this work is that, with coupling matrix synthesis, it is possible to design and manufacture advanced x-coupled bandpass filters in just one iteration, and that the obtained results are in excellent agreement with the predicted characteristics.

7. References

1 S.Shin and S.Kanamaluru, “Diplexer Design Using EM and Circuit Simulation Techniques,” *IEEE Microwave Magazine*, Vol. 8, No. 2, April 2007, pp. 77 – 82.

2 R.J.Cameron, "Advanced Coupling Matrix Synthesis Techniques for Microwave Filters," *IEEE Transactions on Microwave Theory and Techniques*, Vol. 51, No. 1, January 2003, pp. 1-10.

3 R.J.Cameron, "General Coupling Matrix Synthesis Methods for Chebyshev Filtering Functions," *IEEE Transactions on Microwave Theory and Techniques*, Vol. 47, No. 4, April 1999, pp. 433-442.

4 J.B.Ness, “A Unified Approach to the Design, Measurement, and Tuning of Coupled-resonator Filters,” IEEE Transactions on Microwave Theory and Techniques, Vol. 46, April 1998, pp. 342-351.

5 R.J. Cameron, C.M. Kudsia, R.R. Mansour, "*Microwave Filters for Communication Systems*," Wiley-Interscience, Somerset, NJ., 2007.

6 J.B. Thomas, "Cross Coupling in Coaxial Cavity Filters: A Tutorial Overview," *IEEE Transactions on Microwave Theory and Techniques*, Vol. 51, No. 4, April 2003, pp. 1368-1376.

7 A.D. Lapidus and C. Rossiter, "Cross-coupling in Microwave Bandpass Filters," *Microwave Journal*, Vol. 47, No. 11, November 2004, pp. 22-46.

8 Carol G. Montgomery, "*Technique of Microwave Measurements*," volume 11, MIT Radiation Laboratory Series. McGraw-Hill, New York, 1947. p. 306.

9 CMS software: Filter and Coupling Matrix Synthesis. Guided Wave Technology ApS, www.gwtsoft.com

10 Ming Yu, "Power Handling Capability for RF Filters," *IEEE Microwave Magazine*, Vol. 8, No. 5, October 2007, pp. 88 – 97.

11 Ansoft HFSS, "3D Full-wave Electromagnetic Field Simulation" www.ansoft.com/products/hf/hfss/

12 CST Microwave Studio, www.cst.com

13 D. Swanson, G. Macchiarella, "Microwave Filter Design by Synthesis and Optimization," *IEEE Microwave Magazine*, Vol. 8, No. 2, April 2007, pp. 55 – 69.